International Journal of Thermal Sciences 134 (2018) 321–336

Contents lists available at ScienceDirect

International Journal of Thermal Sciences

journal homepage: www.elsevier.com/locate/ijts

Implementation of a thermomechanical model to simulate laser heating in shrinkage tissue (effects of wavelength, laser irradiation intensity, and irradiation beam area)

Patcharaporn Wongchadakul[a,**], Phadungsak Rattanadecho[b,*], Teerapot Wessapan[c]

[a] Faculty of Medicine and Public Health, HRH Princess Chulabhorn College of Medical Science, Chulabhorn Royal Academy, Bangkok, 10210, Thailand
[b] Center of Excellence in Electromagnetic Energy Utilization in Engineering (C.E.E.E.), Department of Mechanical Engineering, Faculty of Engineering, Thammasat University (Rangsit Campus), Pathumthani, 12120, Thailand
[c] School of Aviation, Eastern Asia University, Pathumthani, 12110, Thailand

ARTICLE INFO

Keywords:
Laser
Bioheat
Shrinkage tissues
Skin
Thermomechanical model

ABSTRACT

Advancements in the use of laser technology in the medical field have motivated the widespread use of thermal energy to treat a wide variety of diseases and injuries. During laser-induced thermotherapy, the tissue gains heat from laser irradiation and its shape is deformed due to non-uniform temperature distribution. To describe the phenomenon adequately, the mathematical model that considers both heat transfer and mechanical deformation is needed. In this study, the formulation of mathematical model describing coupled heat transfer and mechanical deformation of tissue subjected to laser-induced thermotherapy is numerically implemented. The effects of laser irradiation time, wavelength, laser intensity, laser beam radius and blood perfusion rate on temperature distribution, Von Mises stress distribution, and displacement of the layered skin during laser irradiation are systematically investigated. The values obtained provide an indication of limitations that must be considered in administering laser-induced thermotherapy.

1. Introduction

Given applications ranging from surgery, treatment of skin diseases, and cosmetic dermatology, lasers have become extremely important treatment devices in the field of dermatology. Compared with traditional methods, laser irradiation is more effective and reliable for treating small wounds and for accelerating the recovery process for treating skin conditions. A laser is produced from a device that emits light in wavelength range between 150 and 11,000 nm [1] through a process of optical amplification based on the stimulated emission of electromagnetic radiation. The term laser is an acronym for Light Amplification by Stimulated Emission of Radiation [2], which was first demonstrated by Maiman [3]. Since then, possible laser applications have been investigated in many fields. Biologists and physicians have been involved in designing new methods in which this special light instrument could be efficiently used to replace conventional techniques, as well as to overcome the inherent limitations of classical medical and research techniques. One of the first laser applications is in ophthalmology, which was studied by Zaret et al. [4], just one year after the laser was invented.

In certain medical treatment applications, laser light sources are used to generate thermal effects in tissue. In these treatments, laser-induced thermotherapy can be optimized by maximizing the therapeutic effect and by minimizing unwanted side effects from the rising thermal energy. For example, high temperatures could cause undesired thermal damage in the surrounding pathology. The thermal response of the tissue exposed to laser light depends principally on a number of parameters including the thermal and optical properties of each tissue and the light source [2]. In addition, thermal denaturation of the skin tissue can lead to remarkable changes in mechanical, thermal, and optical properties [5]. In medical treatment applications with light, simulation tools can be used to predict the thermal and mechanical responses of tissue, such that an appropriate laser light dosage and irradiation time for the subject tissue can be determined.

The skin is the largest sense organ in contact with external environment and can respond to stimuli including temperature, touch, vibration, pressure, and pain. These perceptions are consequence of variable combinations of three types of sensory receptor:

* Corresponding author.
** Corresponding author.
E-mail addresses: patcharaporn.pw@gmail.com (P. Wongchadakul), ratphadu@engr.tu.ac.th (P. Rattanadecho).

https://doi.org/10.1016/j.ijthermalsci.2018.08.008
Received 7 December 2016; Received in revised form 4 August 2018; Accepted 5 August 2018

mechanoreceptors for touch, vibration, and pressure; thermal receptors for temperature; and nociceptors for pain. The International Association for the Study of Pain (IASP) defines pain as an unpleasant sensory and emotional experience associated with actual or potential tissue damage, or described in terms of such damage [5]. All the essential functions of nociceptors, as special receptors for the sensation of pain, depend on ion channels [8,9]. These channels are generally converted from a closed to an open state or gated primarily by three types of stimulus, namely, thermal, mechanical, and chemical stimuli with a threshold of 43 °C and about 0.2 Mpa for the thermal and mechanical stimuli, respectively. The field of skin biothermomechanics is highly interdisciplinary in nature such that it involves bioheat transfer, biomechanics, burn damage, and neurophysiology - all of which are related to the sensation of thermal pain. During heating, thermally induced mechanical stress arises due to thermal denaturation of the skin, which results in shrinkage [10]. Then, mechanical and thermal energy are transduced to an ionic current that leads, in turn, to the sensation of nociceptive pain [11]. Consequently, stress, temperature, burn damage, and thermal pain are highly correlated [5]. The modeling of heat transport in skin has been investigated. Thermal modeling of skin is an important tool for investigating the effect of external heat sources and for predicting abnormalities within tissue. Due to its simplicity, the bioheat transfer model introduced by Pennes [12] was highly utilized and has been used by various researchers over the past decade as the governing equation to simulate the transient temperature distribution in tissue during laser-induced thermotherapy [13–28]. Several numerical models of skin heat transfer have been investigated to illustrate the temperature distribution in skin in different treatment conditions [13–15]. Some studies were carried out on heat transfer of the laser-ultrasonic technique in the skin based on the bioheat model [16–18]. The bioheat models of human tissue subjected to electromagnetic field are also studied [19–21]. The investigation of the temperature distribution in the skin tissue model with an embedded vascular system using the bioheat model is the focus of studies by Lee and Lu [22] and Pual et al. [23]. Dua and Chakraborty [24] presented the modeling of the multiple phase change such as on the melting of fat and the vaporization of water content in tissue. Shen and Zhang [25] presented a mathematical model describing the thermo-mechanical interactions in biological tissue at high temperatures. Recently, a numerical simulation for minimizing undesired thermal damage focusing on the surface cooling effect has been implemented [26].

A model for thermal mechanical deformations of skin has also been studied. The precise heat-induced behavior of tissue and shrinkage depends on several factors, including the maximum temperature reached, the irradiation time [27], and the mechanical stress applied to the tissue during heating [28,29]. Garaizar et al. [30] presented a study of the model for deformation effects of skin induced by the thermal and working environment. The researchers used Finite Element Analysis (FEA) to analyze the simulated results. The modeling of thermal-induced mechanical behaviors of soft tissues for thermal ablation is investigated by Li et al. [31]. A method integrating the heating process with thermal-induced mechanical deformations of soft tissues for simulation is presented, and the thermal ablation process is analyzed. Bioheat transfer and constitutive elastic material law under thermal loads and under non-rigid motion dynamics are used to predict thermal-mechanical deformations through the finite difference method. In the same way, Keangin et al. [32] created a computer simulation of liver cancer treated using a microwave coaxial antenna (MCA). The mathematical models consist of a coupled electromagnetic wave equation, a bioheat equation, and a mechanical deformation equation. In numerical simulations, these coupled mathematical models are solved by using an axisymmetric finite element method (FEM) with temperature-dependent thermal and dielectric properties to describe the microwave power absorbed, the specific absorption rate (SAR) distribution, the temperature distribution, and the strain distribution in liver tissue. A three-dimensional discrete skin fibre tissue model was developed by Jor et al. [33]. The macroscopic mechanical response of the tissue is determined. The parameters are fibre density, fiber thickness, and fiber stiffness. In similar earlier work, Larrabee [34], developed a model to study the deformation and mechanical properties of skin, including its viscoelastic properties (hysteresis, creep, and stress relaxation). The mathematical model is used to simulate wound closures such as the ellipse and rectangular advancement flap. Most studies on skin exposure to laser treatment, however, focused on modeling and determining the effects of specific parameters such as wavelength. In contrast, only a few studies would investigate the effect of thermal stress on heat transfer in the layered skin, although the effect of thermal stress will directly affect the therapeutic heat transfer and pain sensation during treatment.

In present study, the deformed layered skin model exposure to laser treatment is numerically modeled. The temperature distribution, Von Mises stress distribution, and displacement are the dependent variables considered given their clinical importance. In the present study, the thermal mechanical deformation model of skin during laser-induced thermotherapy is developed based on a 3-layered skin model. The finite element method (FEM) is applied for modeling numerical simulations in order to analyze temperature changes in layers of skin tissue. The study utilized the energy absorption equation of the laser irradiation described by Beer-Lambert's law and Pennes's bioheat model for spatial transient temperature distribution. Further, the equilibrium equation is used to describe the laser-induced shrinkage phenomenon in skin. This modeling approach is used in deference to ethical considerations: that is, exposing living humans to laser irradiation for experimental purposes must be limited due to the potential risks involved in doing so. It is also more convenient to develop a biological tissue model, including transport processes, through the numerical simulation, as described above.

2. Formulation of the problem

According to the real biological structure, skin is divided into three layers: the epidermis, the dermis, and subcutaneous tissue [35]. In realistic situation, when skin tissue is exposed to laser irradiation, deformation is occurred at the heated positions due to the temperature gradient. In the present work, a 2D axisymmetric thermomechanical skin model is used to study phenomena that occur in the skin layer during subjected to laser thermography. The absorption characteristics and phenomena occurred depend on number of factors, including the optical, thermal, and mechanical properties of skin tissue, as shown in Table 1.

3. Methods and model

The study focuses attention on heat transfer characteristics and mechanical deformation induced in the skin during subjected to laser irradiation in different therapeutic situations. The FEM-based numerical simulation via COMSOL™ Multiphysics, is applied to model the temperature changes and deformation of skin layered skin. In this study, the surface spatial mode of the laser beam is assumed to be Gaussian in nature. The attenuation of laser light in the layered skin described using Beer-Lambert's law. Mechanical deformation of layered skin is described by equilibrium equations. Using this skin thermomechanical model, the temperature and stress history within layered skin tissue is obtained.

3.1. Physical model

A 2D three layer axisymmetric skin model, which is modified from Ref. [36], is employed to determine the temperature distribution and deformation within the target tissue during laser induced thermotherapy process. With this model, the deformation or thermal shrinkage can be predicted directly in term of the thermal characteristics. Fig. 1

Table 1
Thermal properties and optical properties of tissues [15,18,37–41].

	Epidermis	Dermis	Subcutaneous fat
Thickness (mm)	0.05	1.95	10
Tissue density, ρ(kg/m^3)	1200	1090	1210
Specific heat of tissue, C (J/kg.K)	3950	3350	2240
Thermal conductivity, k (W/(m.K))	0.24	0.42	0.194
Blood perfusion, ω_b (1/s)	0	0.0031	0.0031
Metabolic heat generation, Q_{met} (W/m^3)	368	368	368
Thermal expansion coefficient (1/K)	0.0001	0.0001	0.0001
Poisson's ratio (-)	0.48	0.48	0.48
Young's modulus (Mpa)	102	10.2	0.0102
Absorption coefficient, a (1/m), 532 nm (I-II)	0.9	0.24	0.24
Absorption coefficient, a (1/m), 800 nm (I-II)	0.53	0.24	0.24
Scattering coefficient, b (1/m)	5.0		
The width of the irradiated area, σ (mm)	1.0,2.0		
Ambient temperature, T_{am} (°C)	25.0		
Initial temperature, T_0 (°C)	36.0		
Blood temperature, T_b (°C)	36.0		
Heat convection coefficient, h (W/m^2.K)	10.0		
Blood density, ρ_b (kg/m^3)	1060.0		
Specific heat of blood, C_b (J/kg.K)	3660.0		
Intensity, I (W/mm^2)	1.0, 2.0		

shows the 3D and 2D planes of the skin model used in this study. Although the skin comprises of complex heterogeneous tissue, the model used in this study was assumed and constructed in an axisymmetric plane with three distinct layers (epidermis, dermis, and subcutaneous tissue), as shown in Fig. 1(b). It was also assumed that the tissue is approximately uniform, homogeneous and isotropic in the same layer, which means there is no difference in the thermal and optical parameters within any given layer. A collimated laser beam normal to the surface has a small portion of the light reflected at the skin surface and the remaining light is attenuated in the tissue by absorption and scattering. Further, it is assumed that the laser spot is circular and that the laser irradiates the layered skin perpendicularly, where the heat source was confined. Table 1 gives the skin layer thicknesses, thermal properties, optical properties and mechanical properties used in this study, which are taken directly from Chen et al. (2014) [15], Aguilar et al., 2002 [37], Tseng et al., 2009 [38], Bhowmik et al., 2015 [18], Xu et al., 2008 [39], Delalleau et al., 2006 [40] and Hendriks et al., 2006 [41].

3.2. Equations for heat transfer analysis

To investigate the laser–skin interaction process, a model of unsteady heat transfer as well as the initial and boundary conditions are solved simultaneously with the mechanical deformation equation. To simplify the problem, the following assumptions are made:

1. The layered skin tissue is a bio-material with constant thermal properties and optical parameters in the same layer.
2. There is no phase change of substance in the tissue.
3. There is no chemical reaction in the tissue.
4. Two-dimensional model with axisymmetric plane is assumed.
5. Unsteady heat transfer is considered.
6. The contact surface between each tissues is assumed to be smooth condition.
7. All tissues are assumed to be homogeneous and isotropic.
8. Laser deposition term in the tissue is following the Beer-Lambert's law.

The temperature distribution within the layered skin is obtained by solving Pennes's bioheat equation [12]. The transient bioheat equation, which effectively describes how heat transfer occurs within the skin, can be written as

$$\rho C\frac{\partial T}{\partial t} = \nabla\cdot(k\nabla T) + \rho_b C_b \omega_b (T_b - T) + Q_{met} + Q_{Laser} \tag{1}$$

where ρ is the tissue density (kg/m^3), C is the heat capacity of tissue (J/kg K), k is thermal conductivity of tissue (W/m K), T is the tissue temperature (° C), T_b is the temperature of blood (° C), ρ_b is the density of blood (kg/m^3), C_b is the specific heat capacity of blood (J/kg K), ω_b is the blood perfusion rate (1/s), Q_{met} is the metabolism heat generation (W/m^3) and Q_{Laser} is the external heat source term related to laser irradiation (W/m^3).

In the analysis, heat conduction between tissue and blood flow is approximated by the blood perfusion term, $\rho_b C_b \omega_b (T_b - T)$.

3.3. Boundary condition for heat transfer analysis

The axisymmetric plane is shown in Fig. 1(b), and the boundary conditions and the physical domain are indicated in Fig. 2. The upper surface of layered skin (z = 0) is considered a convective boundary condition,

$$-n.(-k\nabla T) = h_{am}(T - T_{am}) \tag{2}$$

where T_{am} is the ambient temperature (°C), h_{am} is the convective coefficient of the air (W/m^2 K).

The outer surface of the skin tissue with the exception of the upper surface is considered as a constant core body temperature (T_c),

$$T_{c=} = 36°C,\ t \geq 0\,s \tag{3}$$

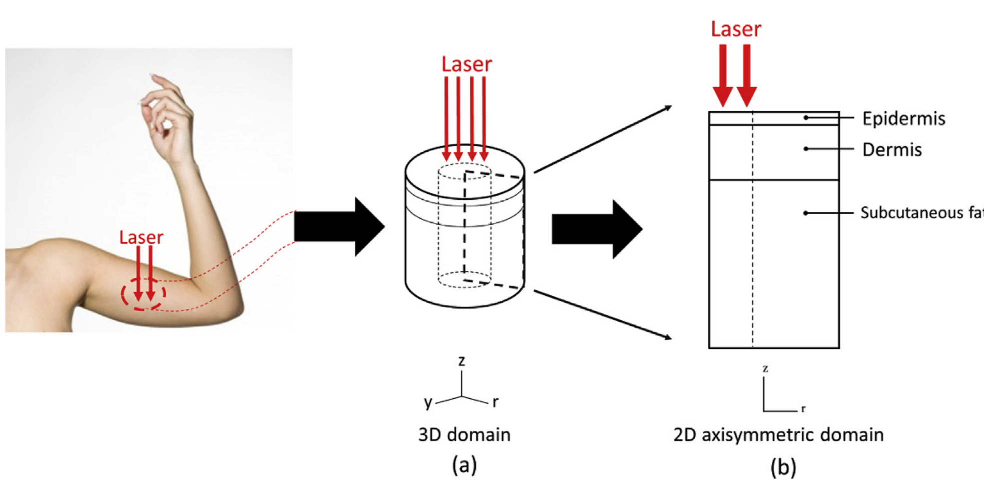

Fig. 1. The skin model, (a) 3D skin model which laser irradiation, (b) 2D skin model which laser irradiation.

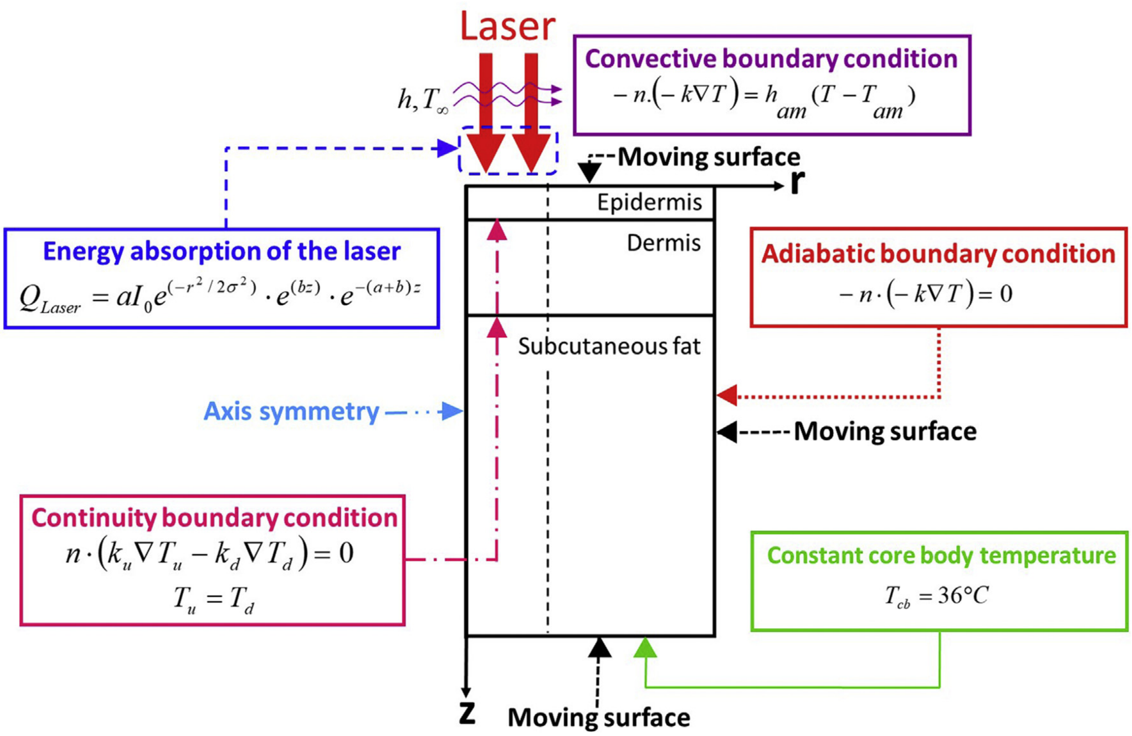

Fig. 2. Boundary conditions and physical domain.

It is assumed that no contact resistance occurs between each internal layer i.e., epidermis, dermis, and subcutaneous tissue. Therefore, the internal boundaries are assumed to be continuity boundary conditions,

$$n{\cdot}(k_u\nabla T_u - k_d\nabla T_d) = 0 \tag{4}$$

The laser irradiation is applied on the top surface of the model. The laser intensity along the tissue depth (z) is described by Beer-Lambert's law as follows:

$$I(z) = I_0e^{(-r^2/2\sigma^2)}.e^{(bz)}.e^{-(a+b)z} \tag{5}$$

The layered skin tissue initially at normal temperature of 36 °C is suddenly taken into exposure to laser irradiation with constant intensity and continuously supplying. The absorption of laser energy within the tissue can be expressed as;

$$Q_{Laser} = aI_0e^{(-r^2/2\sigma^2)}.e^{(bz)}.e^{-(a+b)z} \tag{6}$$

where I is the laser irradiation intensity (W/m^2), I_O is the irradiation intensity at the skin surface (W/m^2), a is the absorption coefficient (1/m), b is the scattering coefficient (1/m), z is the depth of the tissue and σ in eqs (5) and (6) denote as the width of the irradiated area (mm).

3.4. Mechanical deformation analysis

In this study, skin tissue is considered an isotropic material. The model is simplified to a quasi-static model as presented in previous studies [32]. The physical problem of solid mechanics for axisymmetric geometry can be described mathematically using the equilibrium equation (equation (7)), the stress–strain relationship (equation (8)), and the strain displacement relationship (equation (9)) as follows:

$$\begin{aligned}&\frac{\partial\sigma_{rr}}{\partial r} + \frac{\partial\sigma_{rz}}{\partial z} + \frac{\sigma_{rr}-\sigma_{\phi\phi}}{r} + F_r = 0\\ &\frac{\partial\sigma_{rz}}{\partial r} + \frac{\partial\sigma_{zz}}{\partial z} + \frac{\sigma_{rz}}{r} + F_z = 0\end{aligned} \tag{7}$$

$$\begin{aligned}\varepsilon_{rr} &= \tfrac{1}{E}[\sigma_{rr} - \nu(\sigma_{\phi\phi} + \sigma_{zz})] + \varepsilon^{th}\\ \varepsilon_{zz} &= \tfrac{1}{E}[\sigma_{zz} - \nu(\sigma_{\phi\phi} + \sigma_{rr})] + \varepsilon^{th}\\ \varepsilon_{\phi\phi} &= \tfrac{1}{E}[\sigma_{\phi\phi} - \nu(\sigma_{rr} + \sigma_{zz})] + \varepsilon^{th}\\ \varepsilon_{rz} &= \sigma_{rz}(1+\nu)/E\end{aligned} \tag{8}$$

$$\begin{aligned}&\varepsilon_{rr} = \frac{\partial u_r}{\partial r},\ \varepsilon_{zz} = \frac{\partial u_z}{\partial z},\ \varepsilon_{\phi\phi} = \frac{u}{r}\\ &\varepsilon_{rz} = \frac{1}{2}\left(\frac{\partial u_r}{\partial z} + \frac{\partial u_z}{\partial r}\right)\end{aligned} \tag{9}$$

where σ in eqs (7), (8) and (12) denote as the stress (Pa), ε is the strain, F is the external body load (0 here), E is Young's modulus (Pa), ν is the Poisson's ratio and u is the average displacement (m). Further, the thermal strain (ε^{th}) was calculated as follows:

$$\varepsilon^{th} = \int_{T_{ref}}^{T} \alpha dT \tag{10}$$

where T_{ref} = 36°C is the reference temperature and α is the temperature-dependent tissue thermal expansion coefficient (1/°C).

In this study, the lower surface of skin tissue model is set to fixed surface boundary condition. The other sides of the skin tissue are set to the moving surface boundary conditions, and the tissue is deformed as an effect of thermal strain. In addition, the initial stress and strain is set to zero. The initial temperature of skin tissue is 36°C:

$$T_{ref} = 360°C \tag{11}$$

$$\sigma_{ri},\ \sigma_{\phi i},\ \sigma_{zi} \text{ and } \sigma_{rzi} = 0Pa \tag{12}$$

$$\varepsilon_{ri},\ \varepsilon_{\phi i},\ \varepsilon_{zi} \text{ and } \varepsilon_{rzi} = 0 \tag{13}$$

The boundary condition for the mechanical deformation analysis is assumed to be free for all surfaces.

3.5. Calculation procedure

In this study, the bioheat equation, equilibrium equation and related boundary conditions are numerically solved by using FEM via

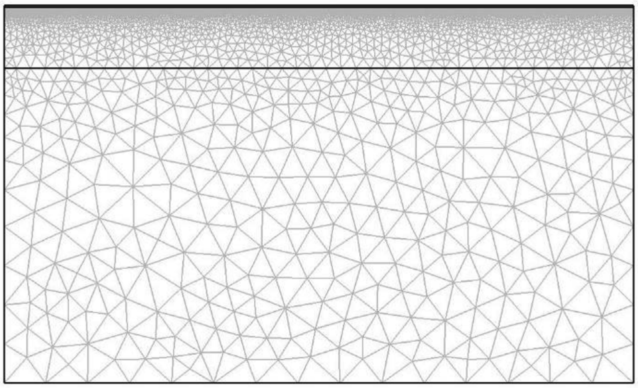

Fig. 3. A two dimensional finite element mesh of human skin model.

COMSOL™ Multiphysics. In addition, the phenomena occurred also depends on the type of skin tissue [42,43]. The simulated results are analyzed by comparing them with simulated results which directly taken from literature in order to verify the accuracy of the developed mathematical model. The model is discretized using triangular elements, as shown in Fig. 3. The convergence test for a wavelength of 532 nm, an intensity of 1.5 W/mm^2, and various properties (Table 1) was performed to identify the number of elements required. The convergence curve resulting from the convergence test is shown in Fig. 4. This convergence test led to a grid with approximately 40,000 elements. It is reasonable to confirm that at this element number the accuracy of the simulation results is independent from the number of elements.

4. Results and discussion

The effects of wavelength, laser irradiation intensity, laser beam radius, irradiation time and blood perfusion rate on the temperature distribution, the Von Mises stress distribution, and the tissue displacement in deformed layered skin tissue during laser-induced thermotherapy were carried out systematically, as shown in Figs. 6–18.

For the simulation, the optical properties and the thermal properties were taken directly from Table 1. We adopted the absorption coefficients of the epidermis, dermis and subcutaneous tissue from Tseng et al. (2009) [38] and Aguilar et al., 2002 [37]. The thermal properties and skin thicknesses are taken from Chen et al. (2014) [15]. The metabolic heat generation is obtained from Bhowmik et al. (2015) [18]. Thermal expansion, Poisson's ratio and Young's modulus are taken from Xu et al. (2008) [39], Delalleau et al., 2006 [40] and Hendriks et al., 2006 [41], respectively, as shown in Table 1.

4.1. Verification of the model

In order to verify the accuracy of the present numerical model, two validation cases have been performed. Fig. 5(a) illustrates the modified case of the simulated results was then validated against the numerical results with the geometric model obtained by He et al. (2004) [44]. The axially symmetrical of two layers of skin tissue with a cancerous tumor was used in the validation case, in which the skin was exposed to laser irradiation at an intensity of 1.4 W/mm^2. The comparison of selected test case results between He et al., 2004's [44] value and present result on temperature distribution value has done.

Fig. 5(b) indicates the axial symmetry layered skin model obtained by Chen et al. (2014) [15], which composes of epidermis, dermis and subcutaneous fat layer. The computerization model is simulated with wavelength of 532 nm and laser power set as 2 W. The temperature values with elapsed times at laser center beam are demonstrated and compared between Chen et al., 2014's [15] values and the present result.

A good agreement of the temperature distribution with elapsed times between the present solution and both of He et al. (2004) [44] and Chen et al., 2014 [15] are clearly shown. This close agreement supports the position that the present numerical model is accurate. It is important to note, however, that some errors may occur in simulations generated by the input thermal properties, the input optical properties, and the numerical scheme.

4.2. Temperature distribution

As explained in the previous section, during laser-induced thermotherapy, a very high temperature could lead to undesired thermal damage in the skin tissue and a sensation of pain arising from thermal and tissue expansion. Therefore, it is necessary to control the extent to which the temperature increases and to limit the hot spot zone. The extent to which the temperature increases during laser-induced thermotherapy depends primarily on the irradiation time, the laser irradiation intensity, and the laser beam radius. In the following discussion, we consider all these parameters.

Figs. 6–9 show the temperature and Von Mises stress patterns in skin

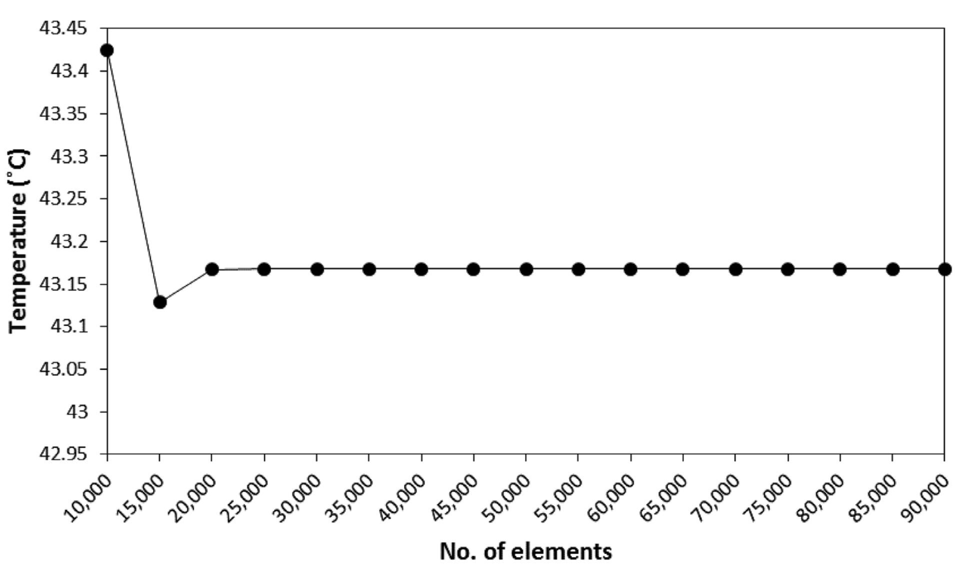

Fig. 4. Grid convergence curve of the model.

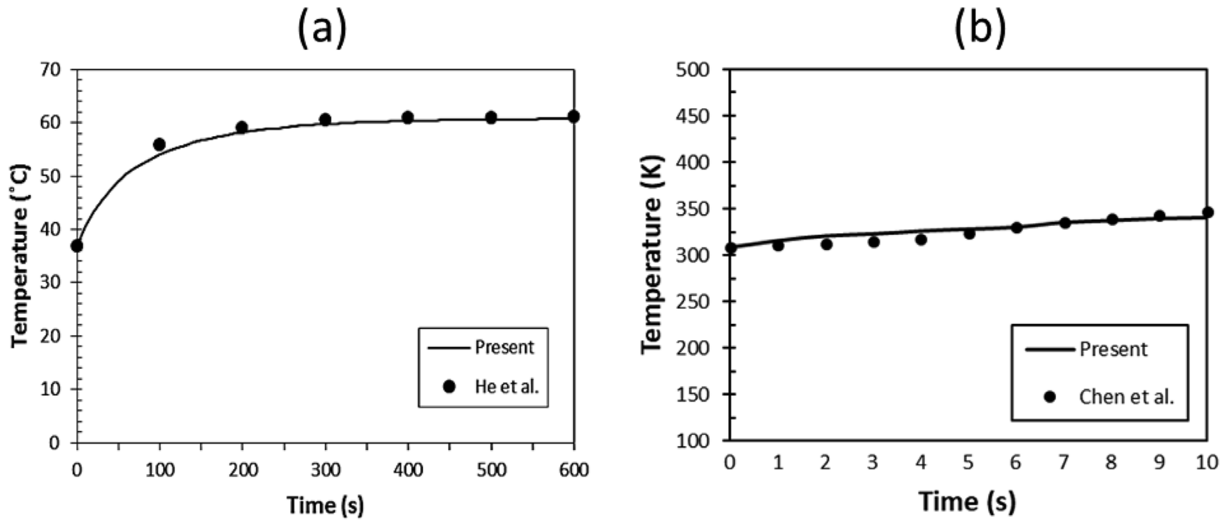

Fig. 5. Comparison of temperature distribution values between the calculated present result and result obtained by (a) He et al., 2004 [44] and (b) Chen et al., 2014 [15].

tissue after a laser-induced thermotherapy process of two wavelengths (532 nm and 800 nm), two intensities (1 W/mm^2 and 2 W/mm^2), and two irradiation times (30 s and 600 s). Fig. 6 shows the temperature and Von Mises stress distribution at wavelengths of 532 nm and 800 nm, laser beam radius of 1 mm and laser intensities of 1 W/mm^2 and 2 W/mm^2, respectively, with irradiation time of 30 s. According to the results, the maximum temperature at a wavelength of 532 nm is on the surface for intensities of both 1 W/mm^2 and 2 W/mm^2 whereas the maximum temperature at a wavelength of 800 nm is inside the tissue. This is because skin tissue has a higher absorption coefficient at wavelength of 532 nm than that at 800 nm. When the skin is exposed to a laser, absorbed energy by skin is converted into thermal energy, which leads to an increase in temperature. However, when the time period increases to 600 s, as shown in Fig. 7, the maximum temperature at a wavelength of 532 nm is moved to inside the tissue, i.e., the subcutaneous fat layer, although a wavelength of 800 nm still occurs in a deeper layer of the skin. This is because thermal conductivity plays an important role in the conductance of the laser energy absorbed by the skin and the irradiation time is long enough for heat to diffuse into a deeper layer.

The effects of laser beam radius and laser intensity are shown in Figs. 8 and 9. Fig. 8 demonstrates the 3D temperature and Von Mises stress distribution at an irradiation time of 600 s, a wavelength of 532 nm. It was found that the greater beam radius led to the maximum temperature position moving up a little bit and also to a higher temperature value. It can clearly be seen that when the laser beam energy is applied at a higher intensity with a laser beam radius of 2 mm, as shown in Fig. 8(g), the maximum temperature position moves up to the upper layer of skin. Fig. 9 shows the 3D temperature and Von Mises stress distribution at a wavelength of 800 nm, a laser intensity of 2 W/mm^2, and an irradiation time 600 s. The simulation results show that for both laser beam radius values, the maximum temperature is reached inside the tissue because of the lower absorption coefficient for a wavelength of 800 nm when compared with wavelength of 532 nm and also the irradiation time is long enough for heat to diffuse into the deeper layer.

Fig. 13 demonstrates the temperature distribution in the layered skin along the radial direction (r-axis and $z = 0$) and the longitudinal direction (z-axis and $r = 0$) at irradiation time of 600 s, at a wavelength of 532 nm and of 800 nm, exposed to a laser irradiation intensity of 1 W/mm^2 and 2 W/mm^2, respectively. Fig. 13 shows that the short wavelength (532 nm) gives rise to the highest center temperature and largest area at this temperature, especially at the center of the leading edge, which is closest to the laser-irradiated beam. This means that for the short wavelength (532 nm) the epidermis absorbs more energy, which it then converts into heat, than is the case for the long wavelength (800 nm). This is due to the effect of the optical properties, i.e., the absorption coefficient of the epidermis layer, the value of which varies with wavelength, and the effect of the thermal parameters of the tissue in each layer vary considerably. In addition, the temperature is higher for both of the wavelengths at a laser intensity of 2 W/mm^2, particularly on the surface, indicating that temperature distribution has a significant effect on laser intensity.

Fig. 14 shows the temperature distribution for two laser wavelength values (532 nm and 800 nm) with two laser beam radius values (1 mm and 2 mm), and a laser intensity of 1 W/mm^2 at an irradiation time of 600 s along the radial (Fig. 13(a)) and longitudinal directions (Fig. 13(b)). The wavelength of 532 nm has a higher temperature than does the wavelength of 800 nm for both laser beam radius values. Moreover, the higher laser beam radius provides a greater irradiation area, which, in turn, results in a higher temperature over a wider region of thermal diffusion than the lower beam radius value does.

Generally, laser-induced thermotherapy relies on two steps: in the early stage of laser-induced thermotherapy, the tissue is heated directly within the optical absorption depth and heat is not diffused very deeply into the tissue. However, over time, heat does diffuse deeper into the tissue. The differences in the temperature fields of the skin tissue in each testing condition are due to the effect of optical properties, i.e., the absorption coefficient value of the epidermis layer, varies with wavelength, and the effects of thermal parameters of the tissue layers vary considerably. In addition, the blood perfusion rate and the cooling of the skin surface, both of which are due to convection, prevents the temperature from increasing even more.

Furthermore, the simulation results suggest that the temperature increase is highest at the irradiation center region, and the temperature would decrease from the irradiation region to the surrounding healthy tissue (for both the radius and the longitudinal directions) for all wavelengths and laser intensity values, after applied laser irradiation. The latter arises because heat from the hot spot zone in the center region diffuses to the surrounding tissue, which constitutes a cold region. In particular, longitudinal temperature distribution affects heat diffusion through the different layers of tissue. It should be noted that the high-temperature area decreases in size as the wavelength increases and that the temperature at the irradiation center region decreases as the wavelength increases. The temperature gradient along the longitudinal direction is greater than that along the radial direction. This is because the upper surface of the skin ($z = 0$) is a convective boundary

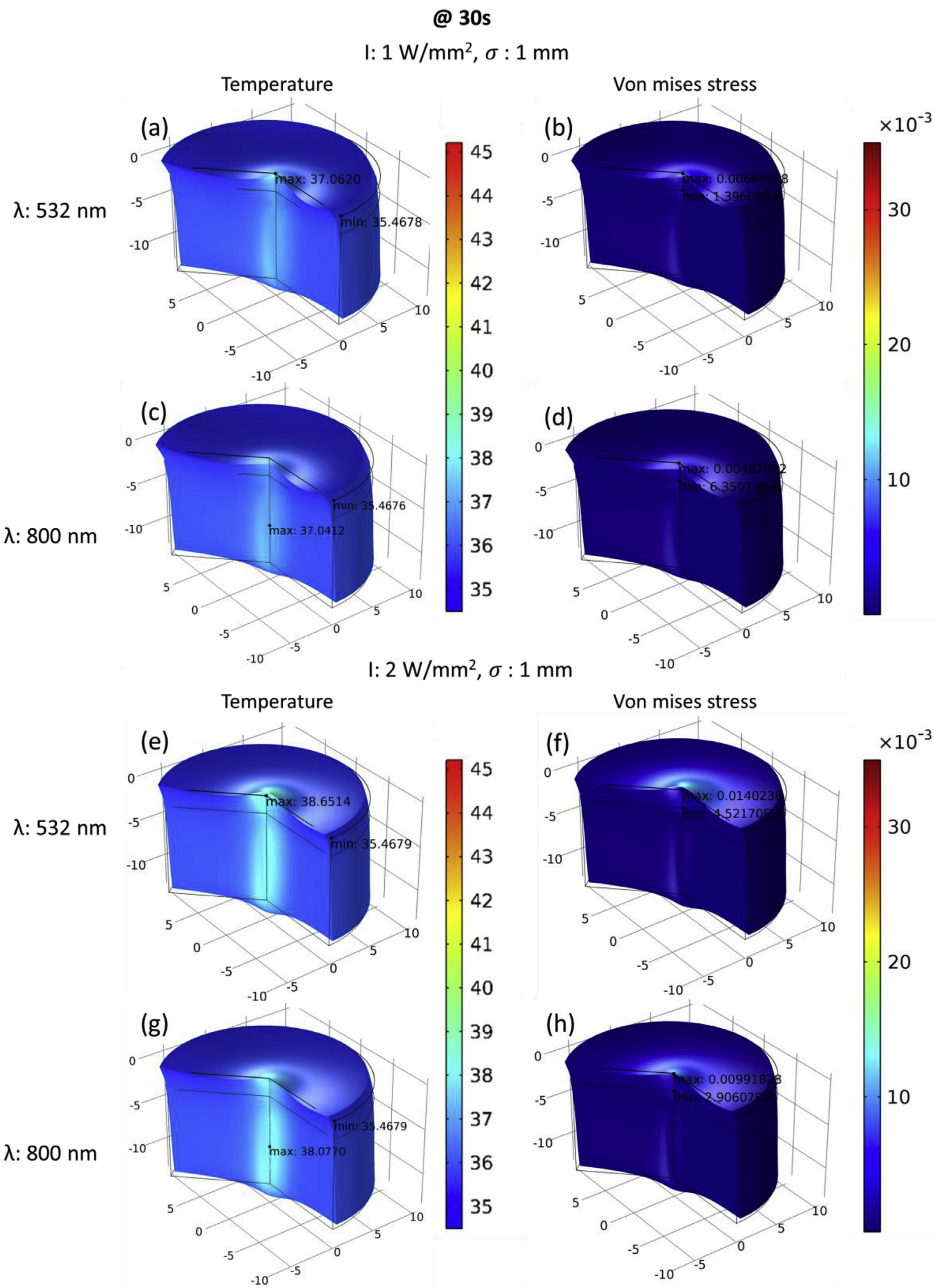

Fig. 6. The 3D temperature and Von Mises stress distribution at wavelengths of 532 nm and 800 nm, intensities of 1 W/mm^2 and 2 W/mm^2, laser beam radius of 1 mm at irradiation time 30 s (a), (c), (e) and (g) Temperature distribution. (b), (d), (f) and (h) Von Mises stress distribution.

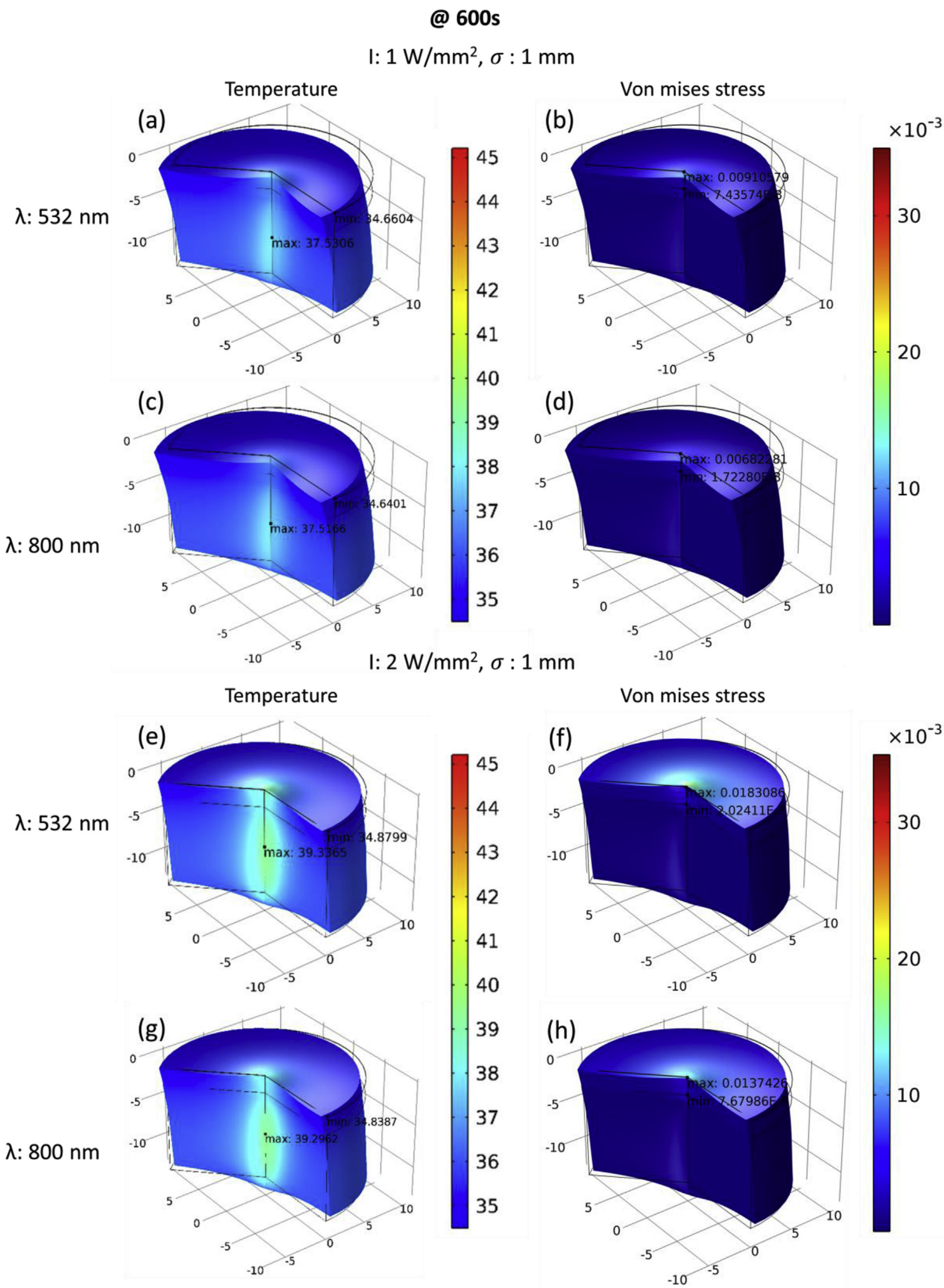

Fig. 7. The 3D temperature and Von Mises stress distribution at wavelengths of 532 nm and 800 nm, intensities of 1 W/mm^2 and 2 W/mm^2, laser beam radius of 1 mm at irradiation time 600 s (a), (c), (e) and (g) Temperature distribution. (b), (d), (f) and (h) Von Mises stress distribution.

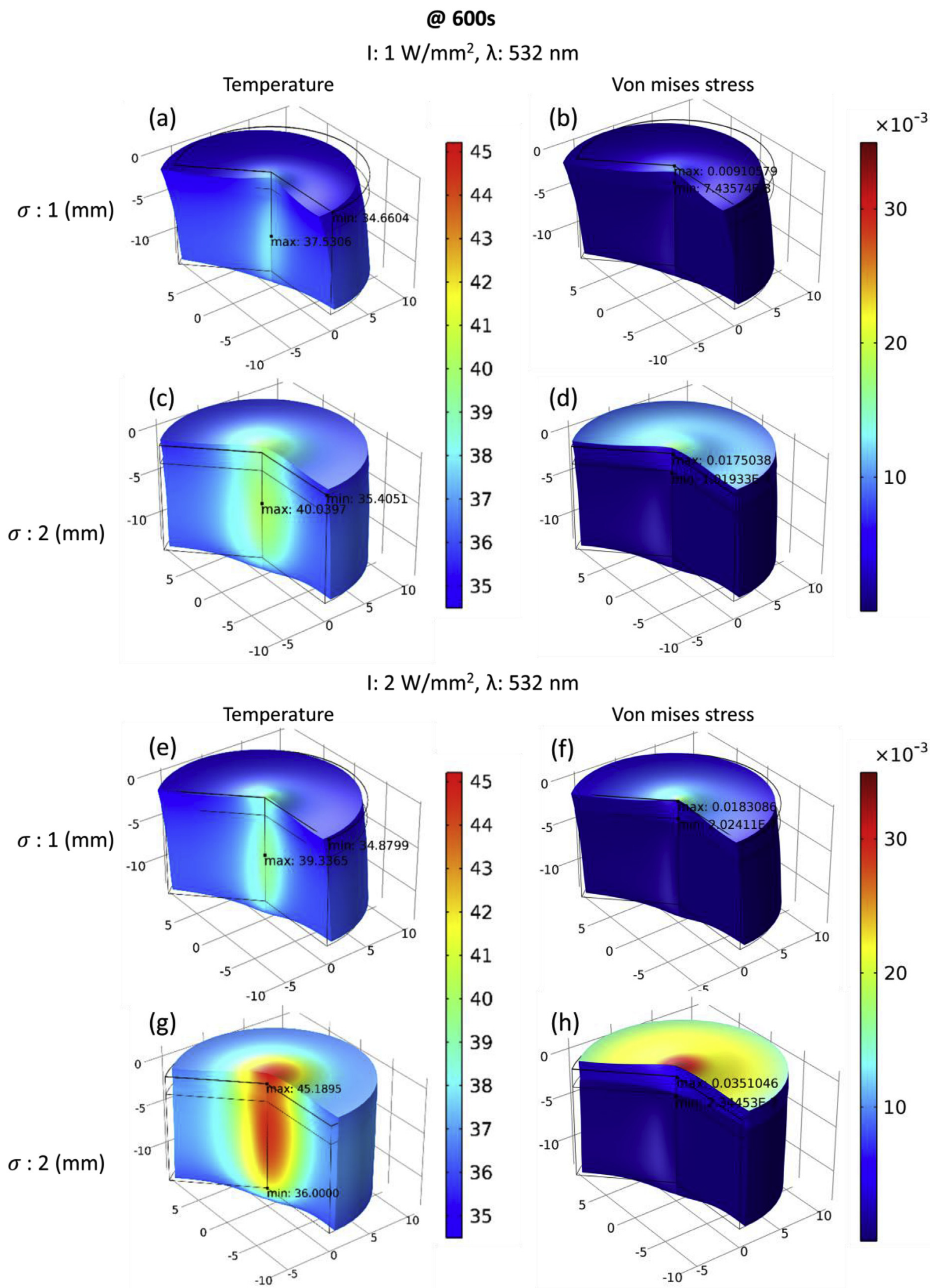

Fig. 8. The 3D temperature and Von Mises stress at wavelength of 532 nm, intensities of 1 W/mm^2 and 2 W/mm^2, laser beam radiuses of 1 mm and 2 mm at irradiation time 600 s (a), (c), (e) and (g) Temperature distribution. (b), (d), (f) and (h) Von Mises stress distribution.

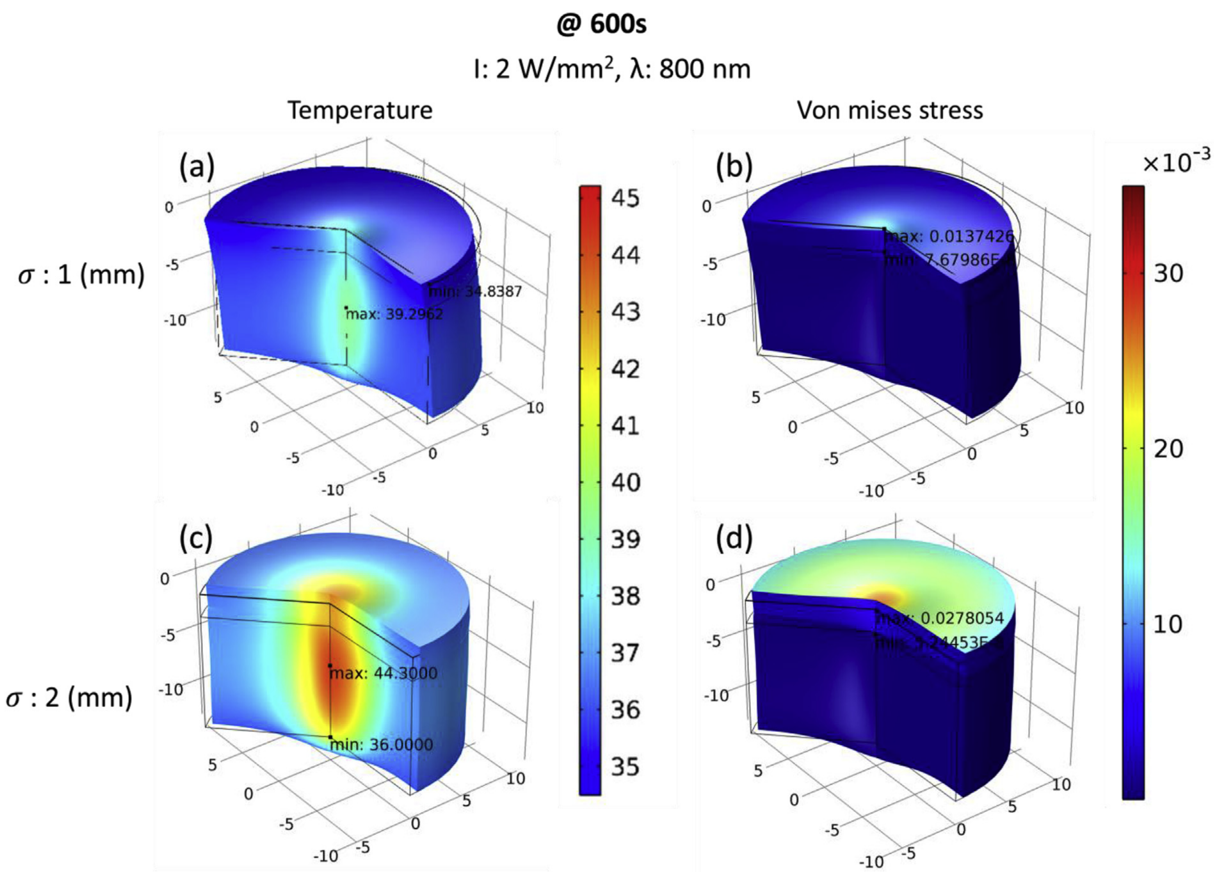

Fig. 9. The 3D temperature and Von Mises stress at wavelength of 800 nm, intensity of 2 W/mm^2, laser beam radiuses of 1 mm and 2 mm at irradiation time 600 s (a) and (c) Temperature distribution. (b) and (b) Von Mises stress distribution.

condition, which continuously conveys heat along the radial direction to surrounding tissue. It could be observed that the increasing intensity level leads to more energy absorption, and causes the temperature increase as well as thermal diffusion, for all wavelengths.

In addition, the discussion on the effect of blood perfusion rate is carried out in Fig. 12. The figure demonstrates temperature distribution of skin after laser irradiation at 532 nm wavelengths, intensities of 2 W/mm^2, laser beam radius of 2 mm at an irradiation time of 30 s, (a)-(b) corresponding to blood perfusion rate at dermis layer of 0.0031 and 0.00031 1/s, respectively. While blood perfusion rate of epidermis and subcutaneous fat layers are still the same for both (a) and (b), which are 0 and 0.0031, respectively. The result illustrates that the blood perfusion rate influenced the temperature change in skin tissue. When increasing the blood perfusion rate of the dermis layer, the temperature decreased because of the consequence of convective heat transfer. To summarize, the relationship between blood perfusion rate and temperature change are inversed.

4.3. Von Mises stress distribution

The simulation results represented in Figs. 6–9 show that the maximum Von Mises stress is positioned on the upper surface of the skin exposed to laser irradiation for all cases whereas the maximum temperature is on either the upper surface of or inside the tissue depending on the condition. A few work have been discussed in this point systematically, in the past.

Fig. 15 indicates the Von Mises stress changes (at $z = 0$ and $r = 0$) with elapsed times at laser wavelengths of 532 nm and 800 nm and a laser intensity of 2 W/mm^2 and a laser beam radius of 1 mm. It can be seen that the wavelength of 532 nm has higher Von Mises stress than the wavelength of 800 nm does. The Von Mises stress with elapsed times for the laser beam radius of 1 mm and the laser beam radius of 2 mm is shown in Fig. 16, with the latter of these showing higher Von Mises stress than the former does. It should be noted that the Von Mises stress approaches a steady state at around 150 s for all conditions and its direction varies with intensity and laser beam radius while reverse variation with the wavelength (as shown in Figs. 6 and 7). Further, these results are related to temperature distribution (as shown in Figs. 6 and 7). By the way, the position of maximum value is different, as also clearly shown in 3D plot in Figs. 6 and 7.

When the Von Mises stress along the radial direction is considered, as shown in Fig. 17(a), it can be seen that the maximum value occurs on the surface of hot spot zone (irradiation center region) and gradually decreases as distance from this surface decreases. However, along the longitudinal direction, the Von Mises stress immediately rises from the maximum value on the surface following deeper distance but not more than 3 mm. In addition, for the Von Mises stress along the radial direction, there is more difference between the two intensities, 1 W/mm^2 and 2 W/mm^2, than is the case in the longitudinal direction.

4.4. Total displacement distribution

The 3D total displacement in layered skin after laser irradiation at a wavelength of 532 nm and 800 nm, an intensity of 1 W/mm^2 and 2 W/mm^2, and a laser beam radius of 1 mm and 2 mm for an irradiation time of 600 s, is shown in Fig. 10. It can be seen that for the laser beam radius of 1 mm, the maximum total displacement is on the edgewise surface of the skin model whether the wavelength is 532 nm or 800 nm, as shown in Fig. 10(a) and (e). But at a higher level of intensity, the position of the maximum total displacement changes to a lower surface, i.e., at the center of the irradiation beam. When the laser beam radius is increased to 2 mm at the same intensity (1 W/mm^2), the maximum total

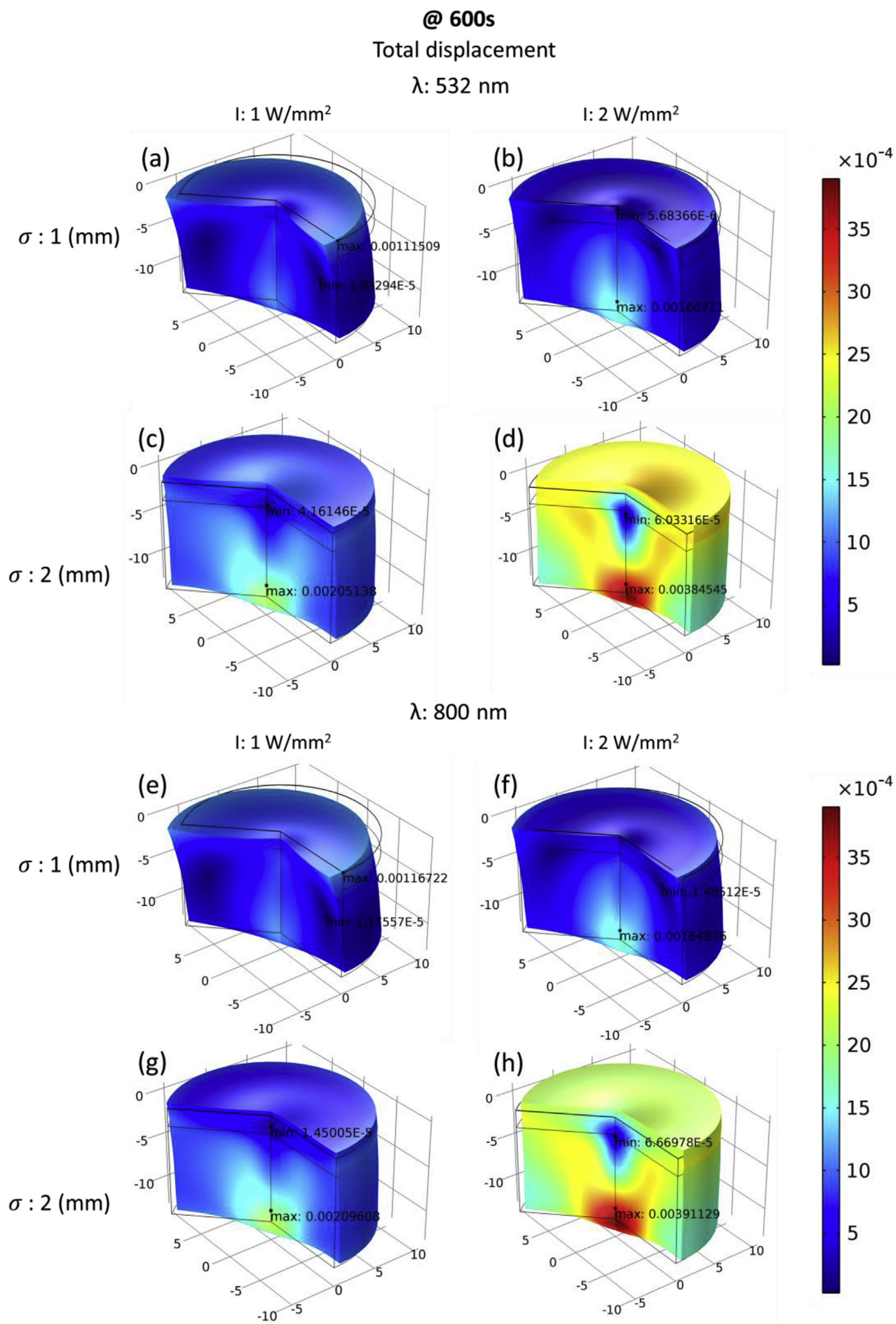

Fig. 10. The 3D total displacement at wavelengths of 532 nm and 800 nm, intensities of 1 W/mm^2 and 2 W/mm^2, laser beam radiuses of 1 mm and 2 mm at irradiation time 600 s (a)–(d) Total displacement of wavelength of 532 nm. (e)–(h) Total displacement of wavelength of 800 nm.

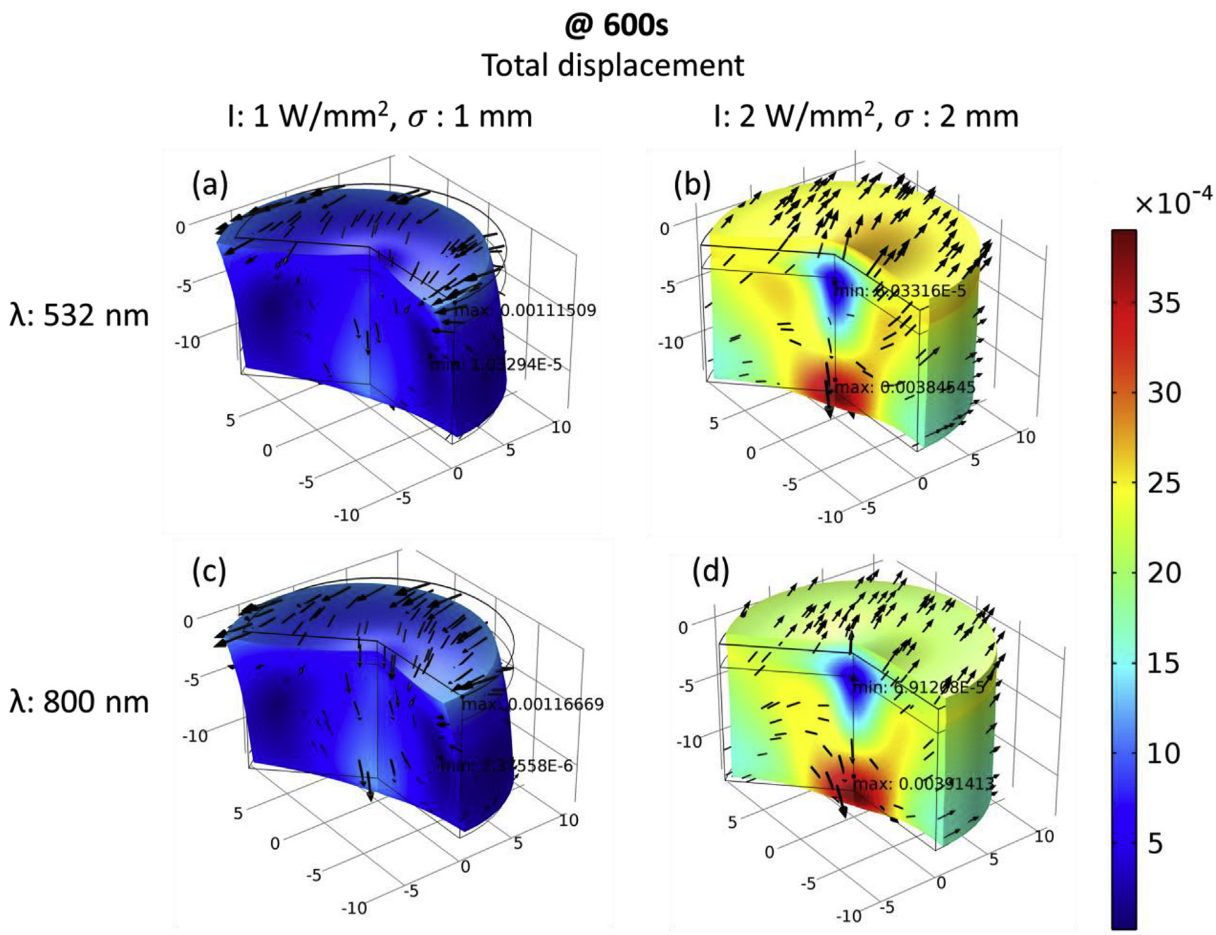

Fig. 11. The 3D total displacement with arrow direction at wavelengths of 532 nm and 800 nm, intensities of 1 W/mm^2 and 2 W/mm^2, laser beam radiuses of 1 mm and 2 mm at irradiation time 600 s (a) and (c) Total displacement at laser beam radius of 1 mm and intensity of 1 W/mm^2. (b) and (d) Total displacement at laser beam radius of 2 mm and intensity of 2 W/mm^2.

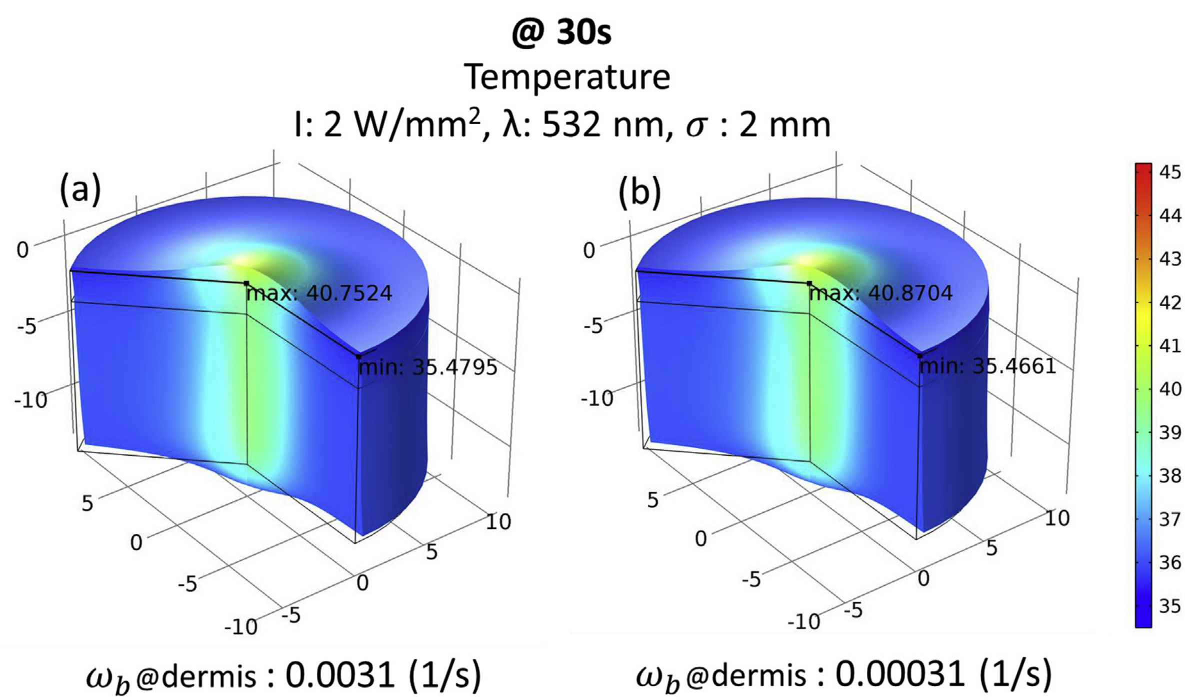

Fig. 12. Temperature distribution of skin after laser irradiation at 532 nm wavelengths, intensities of 2 W/mm^2, laser beam radius of 2 mm at an irradiation time of 30 s (a)–(b) correspond to blood perfusion rate at dermis layer of 0.0031 and 0.00031 1/s, respectively.

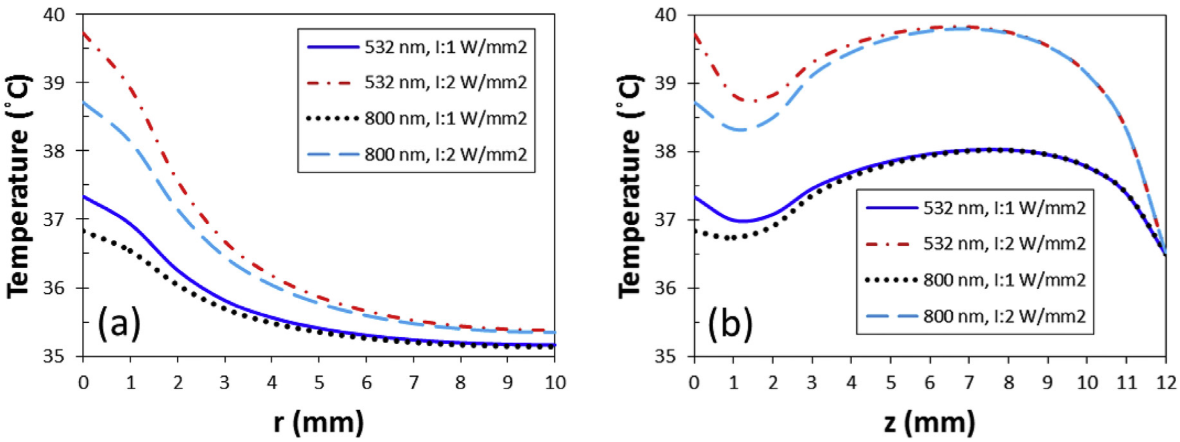

Fig. 13. The temperature distribution of the different laser wavelength (532 nm and 800 nm) and irradiation intensities (1 W/mm^2 and 2 W/mm^2), laser beam radius of 1 mm at irradiation time 600 s (a) and (b) Temperature distribution along radial direction and longitudinal direction, respectively.

displacement position moves to deeper inside the tissue, as shown in Fig. 10(c) and (g). However, with increasing intensity, the position of the maximum value does not change.

The thermomechanism of shrinkage and expansion are also discussed in this section. It should be noted that when skin exposed to laser irradiation, a laser beam radius of 1 mm causes skin to shrink whereas a greater beam radius causes skin to expand, as clearly shown in Fig. 10. The direction of displacement is represented in Fig. 11. In Fig. 11, the vector contours of displacement in case of high laser energy absorption (I = 2 W/mm^2 and σ = 2 mm) display an opposite direction with case of lower laser energy absorption (I = 1 W/mm^2 and σ = 1 mm), especially at the upper surface of layered skin. This is due to the difference of thermal and optical properties and mechanical properties of layered skin during laser-induced thermotherapy process. Moreover, thermally induced stresses due to the gradient temperature as well as non-uniform temperature distributions within skin tissue may also lead to the sensation of thermal pain, in addition to the pain generated by purely heat absorption. This phenomenon should be clearly studied in the future work.

Fig. 18 shows the total displacement (at z = 0 and r = 0) with elapsed times of a laser beam radius of 1 mm and of 2 mm with a laser wavelength of 532 nm and a laser intensity of 2 W/mm^2. It can be seen that the total displacement of the greater laser beam radius (2 mm) is higher than that of the smaller laser beam radius (1 mm). The total displacements along the radial direction and the longitudinal direction

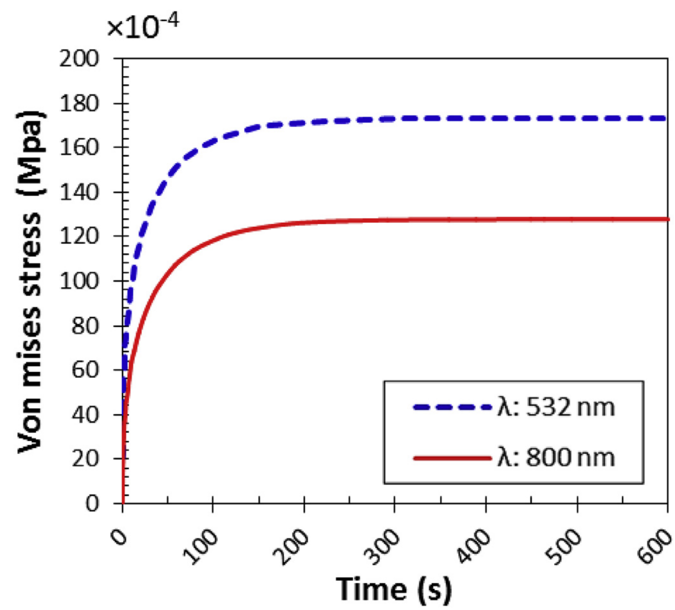

Fig. 15. The Von Mises stress changes (at z = 0 and r = 0) with elapsed times at laser wavelengths of 532 nm and 800 nm, laser intensity of 2 W/mm^2 and laser beam radius of 1 mm.

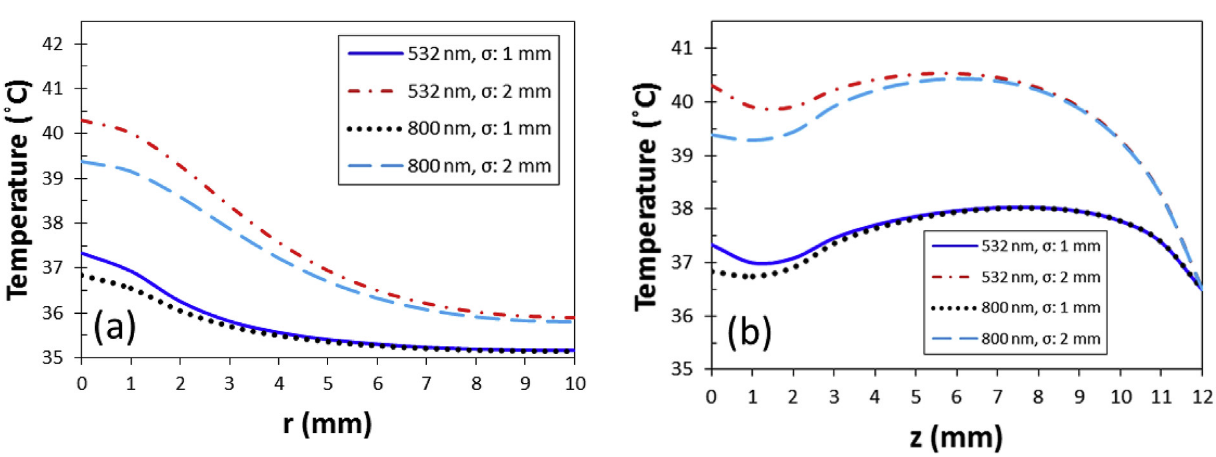

Fig. 14. The temperature distribution of the different laser wavelength (532 nm and 800 nm) and laser beam radius (1 mm and 2 mm), laser intensity of 1 W/mm^2 at irradiation time of 600 s (a) and (b) Temperature distribution along radial direction and longitudinal direction, respectively.

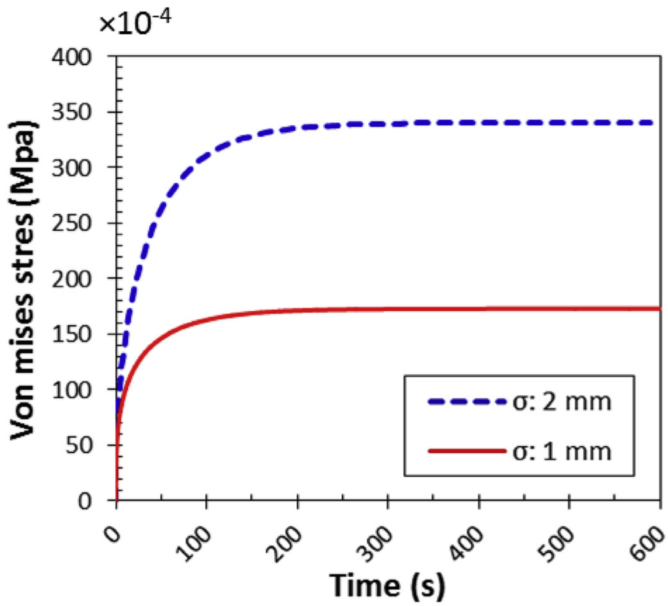

Fig. 16. The Von Mises stress changes (at $z = 0$ and $r = 0$) with elapsed times of laser beam radiuses of 1 mm and 2 mm, laser wavelength of 532 nm and laser intensity of 2 W/mm^2.

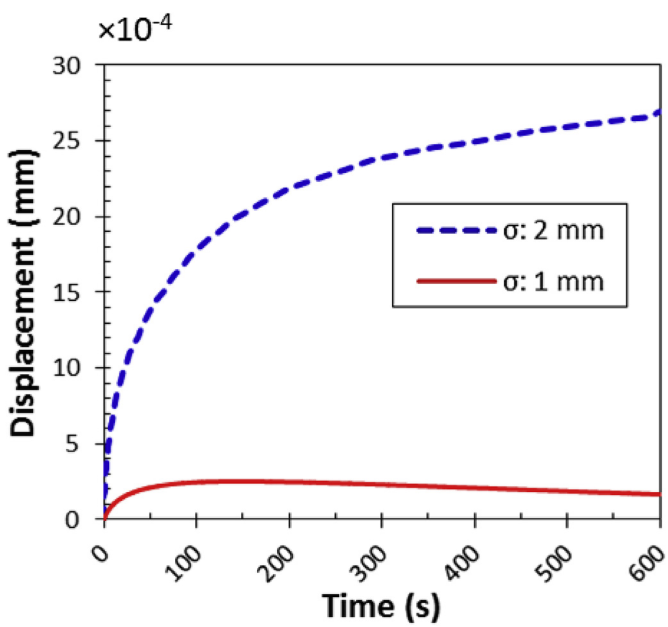

Fig. 17. The Von Mises stress distribution of the different laser intensity (1 W/mm^2 and 2 W/mm^2), laser wavelength of 532 nm, laser beam radius of 1 mm at irradiation time 600 s (a) and (b) Temperature distribution along radial direction and longitudinal direction, respectively.

are shown in Fig. 19. It is shown that along the radial direction, the laser intensity of 1 W/mm^2 engenders greater total displacement than does the laser intensity of 2 W/mm^2. However, along the longitudinal direction, the intensity of 2 W/mm^2 brings about a lower total displacement than does the intensity of 1 W/mm^2 at the leading edge of layered skin. Then, the intensity of 2 W/mm^2 increases to a greater extent than does the intensity of 1 W/mm^2 at z about 3 mm and decreases before reaching the lower surface, at z about 11 mm.

5. Conclusion

A numerical simulation of transient process in layered skin tissue during laser-induced thermotherapy under various treatment conditions was performed, and the result was analyzed. The contour plot of the temperature distribution and Von Mises stress after laser irradiation is clearly shown. It is observed that the heat affected zone during laser irradiation is very localized for all cases, that the applied laser energy is kept low enough to keep the deformation within the thermoelastic regimes, and that vaporization and ablation do not occurs with the maximum temperature at the center of the laser beam. The simulated temperature profile in layered skin tissue is obtained, which is then used as the input for mechanical model. It is found that, at the same stimulus intensity, the Von Mises stress is higher at the surface of skin for all cases. This is because the surface of skin is exposed closer to the laser source. It is expected that the magnitude of skin surface temperature has an effect on the deformation of skin tissue as well as pain.

Furthermore, the results showed that the temperature distribution and laser penetration depth depend strongly on the wavelength, laser irradiation intensity, laser beam radius, and blood perfusion rate. When intensity and irradiation time remain the same, an increased laser wavelength leads to a decrease in the temperature of the skin. Further, the skin's laser energy absorption was shown to be significantly higher in the shorter wavelength range (532 nm) than in the longer wavelength range (800 nm). In addition, the laser intensity has an effect on the extent to which the temperature increases within the tissue: i.e., the higher the intensity value, the higher the temperature within the tissue. Based on the results, a reduced intensity level should lead to a reduction in unwanted thermal injury. Thus, appropriate settings are necessary for treatment to be highly effective and to meet the highest safety standards. Further, it was found that increasing both the laser intensity and laser beam area would result in the skin absorbing more laser energy. Therefore, high laser energy supplied (laser intensity and laser beam area) would provide a higher thermo-mechanical changes, which will directly effect on pain situation. The results also show that irradiation time has a marked influence on the temperature change in skin tissue. Additionally, blood perfusion rate is one of the indicators that influences the temperature change in opposite directions.

The results obtained in the simulation and reported herein contribute to the field's understanding of how to accurately predict temperature and stress distribution in skin tissue during laser induced thermotherapy under different treatment conditions. Nevertheless, in medical treatment, by using the electromagnetic waves; microwave, infrared, laser and similar technologies, various thermotherapy techniques have been developed recently and widely used disease involving skin tissue. However, the problem of pain relief has limited further application and development of thermotherapy treatment. Extensive and detailed researches need to be carried out for thermomechanical model of skin tissue. This study will be helpful for future work on analyzing dermatological implications during exposure to laser irradiation and prediction of therapeutic responses to laser irradiation.

Significant of this work

This study presents the numerical analysis of heat transfer in deformed layered skin model exposed to laser irradiation. The mathematical model combining Pennes's bioheat equation and Beer-Lambert's law are used for all cases. The obtained results contribute to the understanding the effect of related parameters for reduce side effect from hyper-thermal and pre-planning in practical application. Parametric studies on thermal enhanced effects for the laser induced thermotherapy in three layers (epidermis, dermis and subcutaneous fat) by varying the parameters of wavelength, laser irradiation intensities, irradiation beam area and blood perfusion rate disclose more quantitative mechanism for achieving an optimum condition for skin treatment by laser.

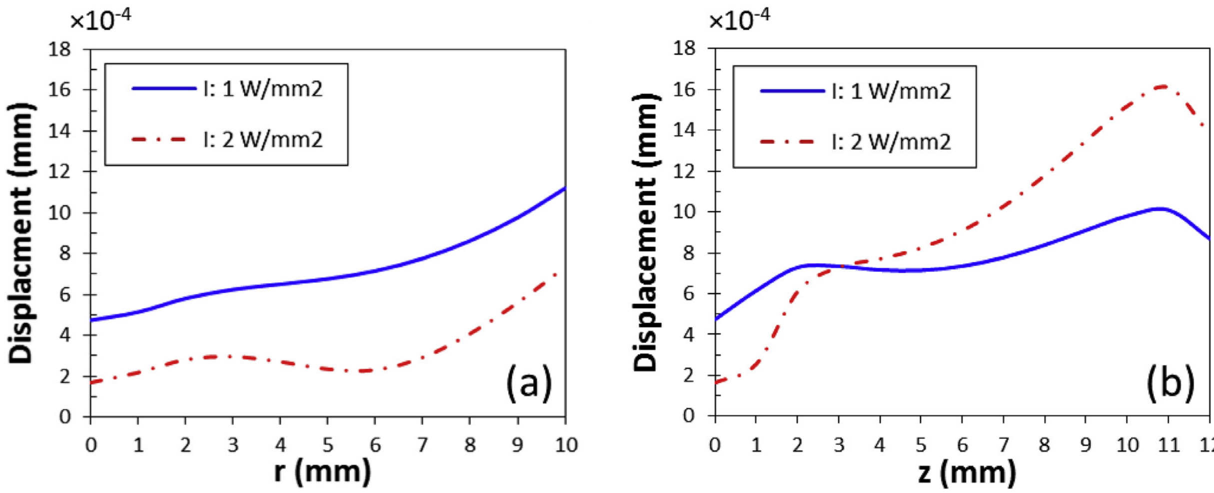

Fig. 18. The total displacement (at $z = 0$ and $r = 0$) with elapsed times at laser beam radiuses of 1 mm and 2 mm, laser wavelength of 532 nm and laser intensity of 2 W/mm^2.

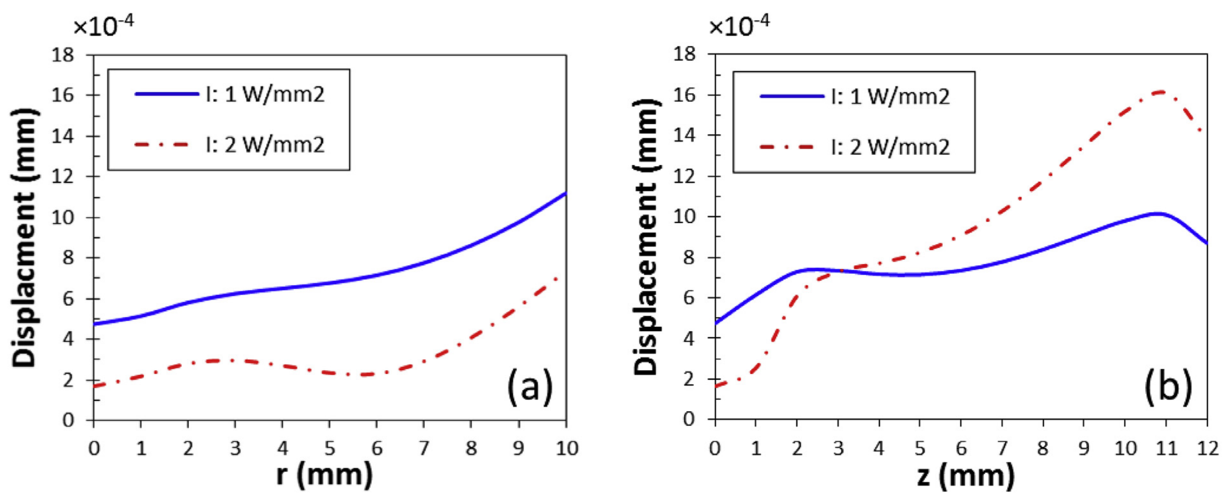

Fig. 19. The total displacement of the different laser intensities (1 W/mm^2 and 2 W/mm^2), laser wavelength of 532 nm and laser beam radius of 1 mm at irradiation time of 600 s (a) and (b) Temperature distribution along radial direction and longitudinal direction, respectively.

Acknowledgements

The Thailand Research Fund (Contract No. RTA 5980009) and The Thailand Government Budget Grant provided financial support for this study.

References

[1] R.G. Gould, The laser. Light amplification by stimulated emission of radiation, The Ann Arbor Conference on Optical Pumping, The University of Michigan, 1959, p. 128.

[2] L. Carroll, T.R. Humphreys, Laser-tissue interactions, Clin. Dermatol. 24 (1) (2006) 2–7.

[3] T. Maiman, Optical and microwave-optical experiments in ruby, Phys. Rev. Lett. 4 (1960) 564–566.

[4] M.M. Zaret, G.M. Breinin, H. Schmidt, H. Ripps, I.M. Siegel, L.R. Solon, Ocular lesions produced by an optical maser (laser), Science 134 (1960) 1525.

[5] F. Xu, T. Lu, Introduction to Skin Biothermomechanics and Thermal Pain, Science Press Beijing and Springer-VerlagBerlin Heidelberg, 2011.

[8] M.J. Caterina, D. Julius, Sense and specificity: a molecular identity for nociceptors, Curr. Opin. Neurobiol. 9 (5) (1999) 525–530.

[9] E.W. McCleskey, M.S. Gold, Ion channels of nociception, Annu. Rev. Physiol. 61 (1999) 835–856.

[10] Y.C. Fung, Biomechanics: Mosion, Flow, Stress, and Growth, Springer-Verlag, New York, 1990.

[11] C.S. Sherrington, The Integrative Action of the Nervous System, Scribner, New York, 1906.

[12] H.H. Pennes, Analysis of tissue and arterial blood temperatures in the resting human forearm (reprint of 1948 article), J. Appl. Physiol. 85 (1998) 5–34.

[13] M. Jaunich, S. Raje, K. Kim, K. Mitra, Z. Guo, Bio-heat transfer analysis during short pulse laser irradiation of tissues, Int. J. Heat Mass Tran. 51 (23–24) (2008) 5511–5521.

[14] E.Y.K. Ng, H.M. Tan, E.H. Ooi, Prediction and parametric analysis of thermal profiles within heated human skin using the boundary element method, Phil. Trans. R. Soc. A 368 (2010) 655–678.

[15] K. Chen, Y. Liang, W. Zhu, X. Sun, T. Wang, Simulation of temperature in skin under laser irradiation with different wavelengths, Optica 125 (2014) 1676–1679.

[16] J.L. Hans, R.S.M. Inder, G. Peter, Bar, H.S. Michael, M. Dieter, Intense focused ultrasound: evaluation of a new treatment modality for precise microcoagulation within the skin. American society for dermatologic surgery, Dermatol. Surg 34 (2008) 727–734.

[17] C. Li, S. Li, Z. Huang, W. Xu, Skin thermal effect by FE simulation and experiment of laser ultrasonics, Appl. Mech. Mater. 24–25 (2010) 281–286.

[18] A. Bhowmik, R. Repaka, S.C. Mishra, K. Mitra, Thermal assessment of ablation limit of subsurface tumor during focused ultrasound and laser heating, J. Therm. Sci. Eng. Appl. 8 (1) (2015).

[19] T. Wessapan, S. Srisawatdhisukul, P. Rattanadecho, Numerical analysis of specific absorption rate and heat transfer in the human body exposed to leakage electromagnetic field at 915 MHz and 2450 MHz, ASME J. Heat Transfer 133 (2011) 051101.

[20] T. Wessapan, P. Rattanadecho, Numerical analysis of specific absorption rate and heat transfer in human head subjected to mobile phone radiation, ASME J. Heat Transfer 134 (2012) 121101.

[21] T. Wessapan, P. Rattanadecho, Specific absorption rate and temperature increase in human eye subjected to electromagnetic fields at 900 MHz, ASME J. Heat Transfer 134 (2012) 091101.

[22] S.L. Lee, Y.H. Lu, Modeling of bioheat equation for skin and a preliminary study on a noninvasive diagnostic method for skin burn wounds, Burns 40 (2014) 930–939.

[23] A. Paul, A. Narasimhan, F.J. Kahlen, S.K. Das, Temperature evolution in tissues

embedded with large blood vessels during photo-thermal heating, J. Therm. Biol. 41 (2014) 77–87.
[24] R. Dua, S. Chakraborty, A novel modeling and simulation technique of photo–-thermal interactions between lasers and living biological tissues undergoing multiple changes in phase, Comput. Biol. Med. 35 (2005) 447–462.
[25] W. Shen, J. Zhang, Skin thermal injury prediction with strain energy, Math. Comput. Model. 41 (2005) 1251–1265.
[26] R. Singh, K. Das, S.C. Mishra, J. Okajima, S. Maruyama, Minimizing tissue surface overheating using convective cooling during laser-induced thermal therapy: a numerical study, J. Therm. Sci. Eng. Appl. 8 (1) (2015).
[27] J.C. Allian, L.M. Le, S.L. Cohen, et al., Isometric tensions developed during the hydrothermal swelling of rat skin, Connect. Tissue Res. 7 (3) (1980) 127–133.
[28] S.S. Chen, N.T. Wright, J.D. Humphrey, Heat-Induced changes in the mechanics of a collagenous tissues: Isothermal, Isotonic Shrinkage J. Biomech. Eng 120 (3) (1998) 382–388.
[29] L. Antunes, K. Montagne, N. Weinbreck, et al., Possible role of tissue shrinkage in high temperature antigen retrieval, Histopathology 48 (4) (2005) 471–473.
[30] O.R. Garaizar, L. Qiao, N. Anwer, L. Mathieu, Integration of thermal effects into tolerancing using skin model shapes, Procedia, CIRP 43 (2016) 196–201.
[31] X. Li, Y. Zhong, R. Jazar, A. Subic, Thermal-mechanical deformation modelling of soft tissues for thermal ablation, Bio Med. Mater. Eng. 24 (6) (2014) 2299–2310.
[32] P. Keangin, T. Wessapan, P. Rattanadecho, Analysis of heat transfer in deformed liver cancer modeling treated using a microwave coaxial antenna, Appl. Therm. Eng. 31 (2011) 3243–3254.
[33] J.W. Jor, M.P. Nash, P.M. Nielsen, P.J. Hunter, Modelling the mechanical properties of human skin: towards a 3D discrete fibre model, Conf. Proc. IEEE Eng. Med. Biol. Soc (2007) 6641–6644.
[34] W.F. Larrabee Jr., A finite element model of skin deformation. Biomechanics of skin and soft tissue: a review, Laryngoscope 96 (4) (1986) 399–405.
[35] G.F. Odland, L.A. Goldsmith, Structure of the Skin, Physiology, Biochemistry and Molecular Biology of the Skin, Oxford University Press, 1991.
[36] C. Li, S. Li, Z. Huang, W. Xu, Skin thermal effect by FE simulation and experiment of laser ultrasonics, Appl. Mech. Mater. 24–25 (2010) 281–286.
[37] G. Aguilar, S.H. Diaz, E.J. Lavernia, J.S. Nelson, Cryogen spray cooling efficiency: improvement of port wine strain laser therapy through multiple-intermittent cryogen spurts and laser pulses, Lasers Sur. Med 3 (2002) 27–35.
[38] S. Tseng, P. Bargo, A. Durkin, N. Kollias, Chromophore concentrations, absorption and scattering properties of human skin in vivo, Optic Express 17 (2009) 14599–14617.
[39] F. Xu, T. Wen, K. Seffen, T. Lu, Modeling of skin thermal pain: a preliminary study, Appl. Math. Comput. 205 (2008) 37–46.
[40] A. Delalleau, G. Josse, J.M. Lagarde, H. Zahouani, J.M. Bergheau, Characterizationof the mechanical properties of skin by inverse analysis combined with the indentation test, J. Biomech. 39 (9) (2006) 1603–1610.
[41] F.M. Hendriks, D. Brokken, C.W. Oomens, D.L. Bader, F.P. Baaijens, The relative contributions of different skin layers to the mechanical behavior of human skin in vivo using suction experiments, Med. Eng. Phys. 28 (3) (2006) 259–266.
[42] L. Fodor, et al., Aesthetic Applications of Intense Pulsed Light, Springer-Verlag London Limited, 2011.
[43] T.S. Alster, J.R. Lupton, Lasers in dermatology. An overview of types and inications, Clin. Dermatol. 2 (2001) 291–303.
[44] Y. He, S. Minoru, K. Ryu, R. Himeno, T. Kawamura, Numerical and experimental study on the human blood circulation and heat transport phenomena thermoregulation in the periphery and hyperthermia-induced tumor blood flow, Computational Biomechanics. RIKEN Symposium, 2004, pp. 97–119 (in Japanese).